Modelling of a Sensorless Rotor Flux Oriented BLDC machine

Conference Paper · October 2017

DOI: 10.1109/EDPE.2017.8123232

3 authors, including:

Kris Scicluna
Malta College of Arts, Science & Technology
62 PUBLICATIONS **160** CITATIONS
SEE PROFILE

Jeremy Scerri
Malta College of Arts, Science & Technology
29 PUBLICATIONS **60** CITATIONS
SEE PROFILE

DRAFT COPY OF FINAL VERSION ACCEPTED AT
International Conference on ELECTRICAL DRIVES and
POWER ELECTRONICS, DUBROVNIC 2017

Modelling of a Sensorless Rotor Flux Oriented BLDC machine

M. Mariano, K. Scicluna, J. Scerri
Institute of Engineering and Transport, Electrical and Electronics
Malta College for Arts, Science and Technology

***Abstract*— This paper presents the modelling and simulation of a low-power Brushless DC machine in a Rotor Flux Oriented mode in MATLAB/Simulink. The modelling of the machine is presented in the synchronous dq-frame. Using this model suitable Proportional Integral controllers have been designed for the Rotor Flux Oriented speed and current loops. Sensorless simulation estimates obtained from a back-emf observer for both electrical angle and rotor speed are presented. The dynamic response of the model is also shown in sensorless closed-loop whereby the estimates obtained are used for control purposes. The errors in the estimated position and speed during closed-loop are kept below 1.9 % and 0.1 % respectively such that the speed controlled system designed and simulated remains stable.**

Keywords—BLDC; Modelling, Simulink; sensorless;

I. Introduction

The Brushless DC (BLDC) machine has been widely used in applications where high-speed and low maintenance are critical requirements. Such applications include unmanned vehicles [1, 2], automotive [3, 4] and aerospace [5, 6]. Typically, closed-loop control of BLDC machines requires shaft speed/position measurements. While these can be obtained through dedicated sensors such as encoders and tachogenerators, such an approach is not usually feasible due to limited application area and cost.

Hence BLDC machine controllers are usually integrated with sensorless speed/position estimation algorithms. Sensorless algorithms are subdivided into two main categories: model based and non-model based. Model based sensorless algorithms estimate the speed/position of the machine through electrical or mechanical models and are particularly suited for high speed operation [7, 8]. Non-model based algorithms are used at close to zero speeds and rely on the injection of additional carrier signals to the fundamental ones required for control [9, 10]. In speed controlled systems such as the one modelled in this paper the back-emf of the BLDC is usually sufficient for accurate speed/position estimates to be used for sensorless closed-loop purposes.

In low-cost Electronic Speed Controllers (ESCs) used with low to medium power BLDC machines a six-step commutation sequence is used [11]. In this method one of the three phases of the machine is left floating allowing for a back-emf voltage measurement. The drawback of the six-step approach is that it has high harmonic content which would result in higher power losses [12]. Since the aim of this paper is to model and simulate a low power BLDC machine in MATLAB/Simulink for battery powered applications; a Rotor Flux Oriented (RFO) control topology was used. This assumes a Pulse Width Modulation (PWM) driven inverter instead of the six-step commutation approach. Therefore, the back-emf has to be estimated through current measurements rather than measured directly through the floating phase.

In Section II the modelling of the BLDC in the synchronous dq-frame is presented. The equations for the stator voltages in terms of physical machine parameters and measurements are shown. These were used for the design of the dq current control loops. Similarly, the mechanical dynamics were used to design the speed control loop. In Section III the design of the back-emf sensorless observer is presented along with the derivation of the estimated electrical angle from estimated back-emf quantities. In Section IV the performance of the model in sensorless closed-loop is shown.

II. Rotor Flux Oriented Modelling

A. Modelling of the BLDC in the DQ-Frame

The mathematical model for vector control presented in this paper assumes that the synchronous frame d-axis is oriented on the rotor flux. This approach has been widely used to control synchronous machines and has been shown to be robust under varying load conditions [13, 14]. Using this representation, the stator voltages in the dq-frame are as expressed in (1) and (2).

$$v_{sd} = \mathrm{R} i_{sd} + \mathrm{L_d} \frac{di_{sd}}{dt} - \omega \mathrm{L_q}\, i_{sq} \quad (1)$$

$$v_{sq} = \mathrm{R} i_{sq} + \mathrm{L_q} \frac{di_{sq}}{dt} + \omega \mathrm{L_d} i_{sd} + \omega \varphi_{\mathrm{rd}} \quad (2)$$

Where:

v_{sd} / v_{sq}	are the stator voltages in the dq-frame
R	is the stator resistance
i_{sd} / i_{sq}	are the stator currents in the dq-frame
$\mathrm{L_d}$/ $\mathrm{L_q}$	are the stator inductances in the dq-frame
ω	is the synchronous frequency
φ_{rd}	is the rotor flux aligned to the d-axis

The mechanical differential equation relating rotor shaft speed to the BLDC electromagnetic torque is expressed in (3).

DRAFT COPY OF FINAL VERSION ACCEPTED AT
International Conference on ELECTRICAL DRIVES and
POWER ELECTRONICS, DUBROVNIC 2017

$$T_e = J\dot{\omega}_m + B\omega_m \quad (3)$$

Where:

T_e	is the electromagnetic torque of the BLDC
J	is the moment of inertia of the BLDC
ω_m	is the rotor speed
B	is the friction coefficient of the BLDC

The necessary parameters used for modelling were based on the experimental BLDC machine shown in Fig. 1 and stated in Table I. Electrical parameters were measured experimentally while mechanical parameters were estimated using dimensional calculations assuming the BLDC as a solid steel cylinder.

Fig. 1. Experimental BLDC used for modelling.

TABLE I. BLDC MACHINE PARAMETERS

Symbol	*Description*	*Value*	*Unit*
P	Power Rating	187	W
V_{rms}	RMS Voltage	11	V
T_{rated}	Rated Load Torque	0.1437	Nm
L_d	'd' frame stator inductance	6.5	mH
L_q	'q' frame stator inductance	6.5	mH
R	Stator Resistance	81.5	mΩ
J	Moment of Inertia	$7.312x10^{-6}$	kg m^2
B	Coefficient of Friction	$6.511x10^{-7}$	-
p	Number of Pole Pairs	14	-
φ_{rd}	Rotor flux aligned to the d-axis	$427x10^{-6}$	Wb

Synchronous inductances L_d and L_q were approximated from the 'abc' stator inductances measured through an LCR meter and assuming a non-salient machine. While the values obtained are not precise they are expected to be accurate within an order of magnitude. More accurate values for L_d and L_q can be obtained by measuring the resulting transient responses for step reference currents in the dq-frame with a locked rotor. Such testing was not carried out due to time constraints associated with the project.

B. *Sensored Control of the BLDC*

By applying Laplace transformations to (1), (2) and (3) and using the SISO tool in MATLAB the Proportional-Integral (PI) controllers of the cascaded RFO control topology shown in Fig. 2 were tuned with gains and bandwidths stated in Table II.

TABLE II. CONTROLLER GAINS

Loop	K_p	K_i	*Closed-Loop Bandwidth [rad/s]*	*Damping Ratio*
Current	0.08125	1018.75	$12.5x10^3$	-
Speed	0.25223	111.826	625	0.707

No field weakening is assumed for the operation of the BLDC such that the d-axis reference $i_d^* = 0$ A. Hence the torque of the electrical machine is a function of the q-axis current i_q as shown in (4).

$$T_e = 3pi_q\varphi_{rd} \quad (4)$$

Where:

T_e	is the electromagnetic torque of the BLDC
p	is the number of pole pairs
i_q	is the stator currents in the q axis
φ_{rd}	is the rotor flux aligned to the d-axis

The reference for the q-axis current i_q^* was generated from the error of the speed reference ω_m^* and actual speed ω_m. The outputs of the current PI controllers are the references for the stator voltages in the dq-frame v_{sd}^* and v_{sq}^*. In this simulation, generation of PWM signals from the stator voltage references has not been considered and ideal three phase voltages v_a, v_b and v_c were applied to the model of the BLDC.

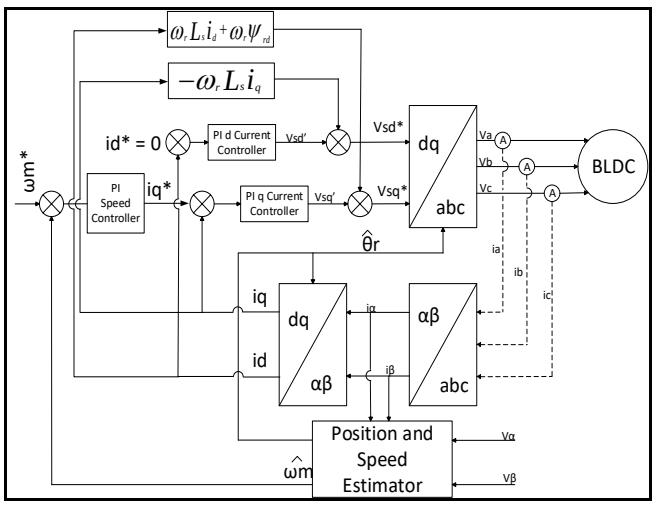

Fig. 2. RFO control of BLDC.

DRAFT COPY OF FINAL VERSION ACCEPTED AT
International Conference on ELECTRICAL DRIVES and
POWER ELECTRONICS, DUBROVNIC 2017

III. Sensorless Position/Speed Estimation

For correct operation of the RFO control topology presented in Section II accurate measurements are required for the rotor position and speed. At high speeds, the electrical angle of the BLDC can be obtained from trigonometry as shown in Fig. 3. Since the vector control algorithm will keep the back-emf vector E_s at an angle of 90° shifted from the d-axis the electrical angle θ_e can be found from the back-emfs in the stationary αβ-frame through equation (5).

$$\theta_e = \tan^{-1}\left(\frac{E_\alpha}{E_\beta}\right) \qquad (5)$$

Where:

θ_e	is the electromagnetic angle
E_α / E_β	are the back-emfs in the αβ-frame

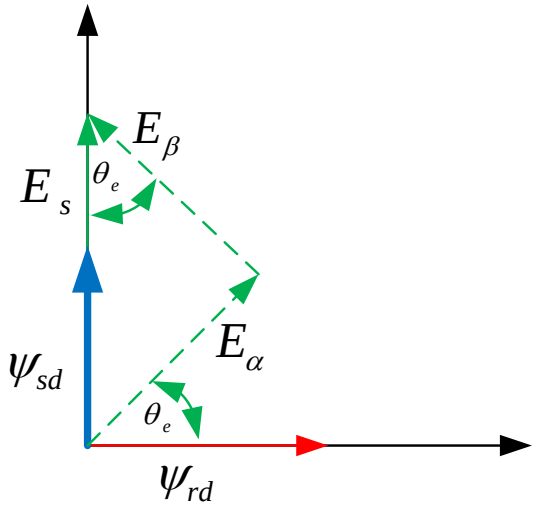

Fig. 3. Caclulation of the electrical angle from back-emf quantities.

As discussed previously in Section I the back-emf quantities required for the estimation of the electrical angle can be obtained through a direct measurement on the floating phase when using the six-step commutation. Another approach which can be used when a floating phase is not available is to estimate E_α and E_β through current measurements i_α and i_β. The actual currents i_α and i_β are compared to estimates generated from the difference of the phase voltages v_α and v_β subtracted from the back-emf estimates as shown in Fig. 4. The errors in the back-emf estimates are compensated with a PI controller such that the estimated currents are made to track the actual currents measured. The calculation of (5) from the estimated back-emf quantities produces the electrical angle estimate $\hat{\theta}_e$ which is differentiated to obtain the estimated electrical frequency $\hat{\omega}$. Successful sensorless closed-loop was obtained with the tracking PI gains set at $K_p = 0.08125$ and $K_i = 4018.75$.

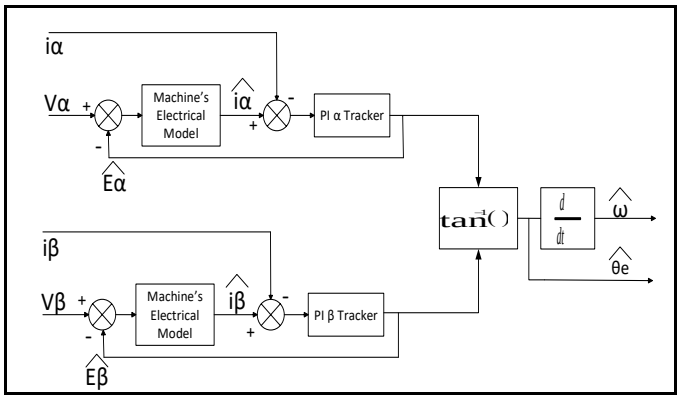

Fig. 4. Model-based sensorless observer for BLDC

IV. Simulation Results

The simulation results shown in this section are for the BLDC described in Section II. The Simulink BLDC machine model is shown in Model A while the model-based observer model is shown in Model B. A reference speed of 400 rad/s (3820 rpm) was used. A constant rated load torque of 0.1437 Nm is applied at the output shaft of the BLDC. The BLDC is started from 0 rad/s up to a preset value in open-loop at which the back-emf is of sufficient magnitude for estimation purposes. The sensorless speed and position estimates are used for sensorless closed-loop control after 0.2 s. Simulation results for the actual/estimated electrical angles required for vector control purposes are shown in Fig. 5 while the error between these two quantities is shown in Fig. 6. The reference/actual rotor speeds are shown in Fig. 7. The actual and estimated currents in the αβ-frame are shown in Figs. 8 and 9 respectively. The estimated back-emfs from which the electrical angle is calculated are shown in Fig. 10. The synchronous frame dq currents are shown in Fig. 11.

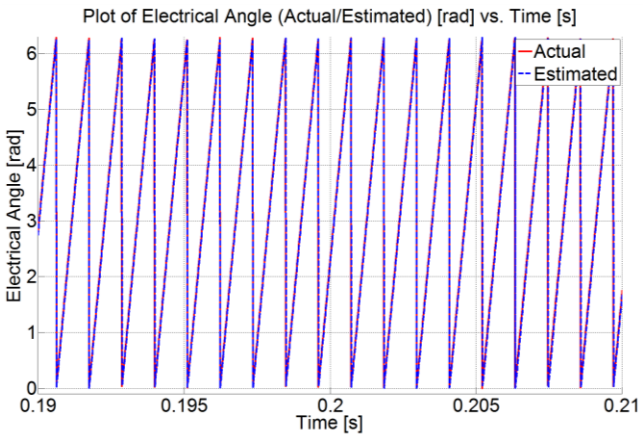

Fig. 5. Plot of Electrical Angle [rad] vs. Time [s] with Load Torque of 0.1437 Nm and sensorless changeover at t=0.2 s.

DRAFT COPY OF FINAL VERSION ACCEPTED AT
International Conference on ELECTRICAL DRIVES and
POWER ELECTRONICS, DUBROVNIC 2017

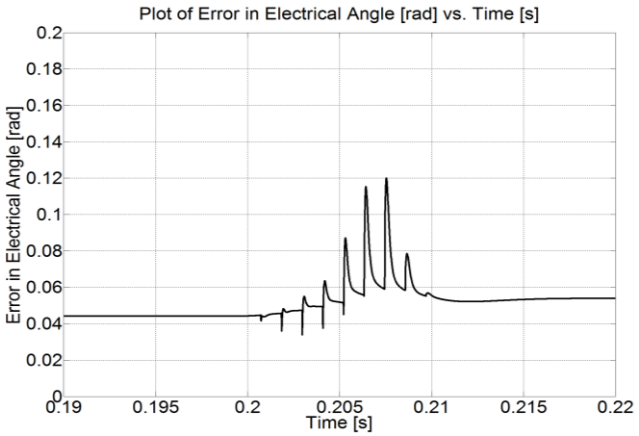

Fig. 6. Plot of Error in Electrical Angle [rad] vs. Time [s] with Load Torque of 0.1437 Nm and sensorless changeover at t=0.2 s.

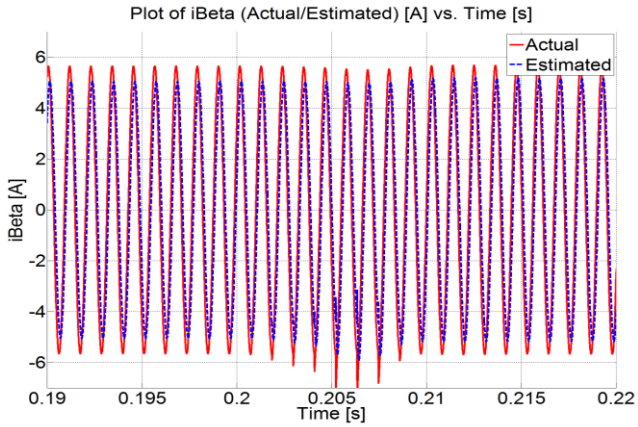

Fig. 9. Plot of i_β [A] vs. Time [s] with Load Torque of 0.1437 Nm and sensorless changeover at t=0.2 s.

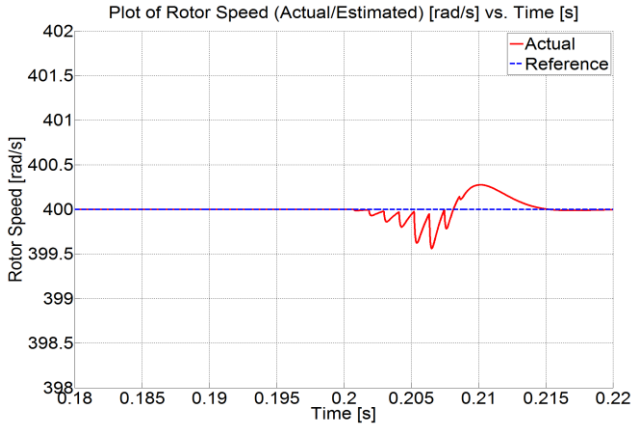

Fig. 7. Plot of Rotor Speed [rad/s] vs. Time [s] with Load Torque of 0.1437 Nm and sensorless changeover at t=0.2 s.

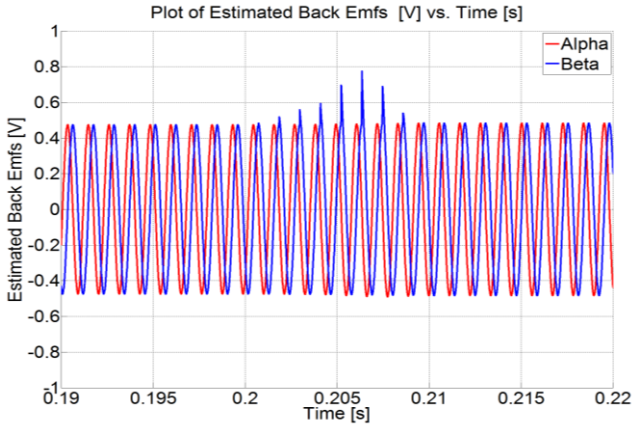

Fig. 10. Plot of Estimated E_α/E_β [V] vs. Time [s] with Load Torque of 0.1437 Nm and sensorless changeover at t=0.2 s.

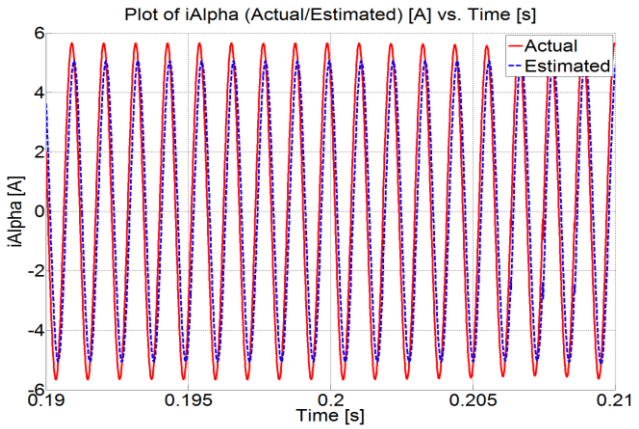

Fig. 8. Plot of i_α [A] vs. Time [s] with Load Torque of 0.1437 Nm and sensorless changeover at t=0.2 s.

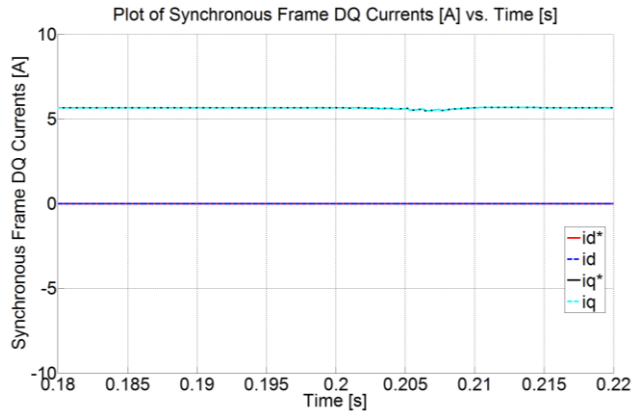

Fig. 11. Plot of i_d/i_q [A] vs. Time [s] with Load Torque of 0.1437 Nm and sensorless changeover at t=0.2 s.

The estimated electrical angle is shown to track the actual electrical angle in Fig. 5. The error in the estimated angle is shown in Fig. 6 and has a maximum value of 0.12 rad (6.87 degrees), which is within 1.9 % of the actual value. The speed control loop is shown to be stable after sensorless changeover at 0.2 s and the maximum error in the actual speed with respect to the reference is 0.4 rad/s (0.1 % of the reference value). Figs. 8 and 9 show that the sensorless estimation loops result in i_α and i_β estimates which are attenuated and phase shifted with respect to the actual quantities; this is expected due to the frequency response of the PI controllers. However, since both α and β quantities are tracked with identical controllers the effects on the estimated electrical parameters are negligible. The estimated back-emfs shown in Fig. 10 are of a sinusoidal nature with transients about the instant of sensorless changeover at 0.2 s. This is a result of the transients on i_β shown in Fig. 9 which are not tracked by the sensorless observer due to the limited bandwidth of the PI tracker. The synchronous frame currents in Fig. 11 show that the d-axis current i_d = 0 A while the q-axis current i_q has a positive value to produce the required torque in the positive direction of motion.

V. Conclusions

This paper has reviewed the modelling of the BLDC machine for vector control purposes in the dq-frame so as to facilitate modelling in MATLAB/Simulink. The stator voltage electrical dynamics and rotor mechanical dynamics were presented in Section II. These equations were required to implement the necessary PI controllers required for speed RFO control of the BLDC machine. A high speed model-based sensorless observer was shown in Section III and the estimation of the electrical angle θ_e discussed. The proposed sensorless observer estimates the back-emf quantities E_α and E_β by comparing estimates for the currents in the αβ-frame i_α and i_β. The tuning of a suitable observer to track these estimates was also presented.

From the simulation results presented in Section IV it was noted that the sensorless observer designed and simulated fails to track current transients in the αβ-frame during sensorless changeover. However, the effect of this limitation associated with the bandwidth of the PI controllers has a negligible effect on the operation of the BLDC as the error in the estimated angle is a maximum of 1.9 % while the error in the actual speed is 0.1 %. The tuning of these PI controllers was set such that a sensorless operation is possible over a wide range of loading conditions. The bandwidth of the observer can theoretically be increased indefinitely to track transients however this will be limited in practice by the sampling and estimation rate of the microcontroller/DSP.

The sensorless observer presented in this paper has the disadvantage of having to estimate back-emf quantities unlike that associated with reading the floating phase in a six-step commutation. However, it has the advantage that it can be used with a PWM inverter for improved efficiency in battery operated applications. From the study presented in this paper it was confirmed that such a model-based observer is more suitable for machines with slower electrical/mechanical dynamics such that transients are physically limited. The advantages of the modelling presented in this paper is that the various controllers within both the cascaded RFO oriented topology and the sensorless observer can be tested and tuned simultaneously for various load conditions. The model was also designed in such a way that it can be modified to simulate and design controllers for machines of different power ratings and saliency types.

References

[1] J. A. Benito, G. Glez-de-Rivera, J. Garrido, and R. Ponticelli, "Design considerations of a small UAV platform carrying medium payloads," in *Design of Circuits and Integrated Systems*, 2014, pp. 1-6.

[2] A. Sanchez, L. García Carrillo, E. Rondon, R. Lozano, and O. Garcia, "Hovering flight improvement of a quad-rotor mini UAV using brushless DC motors," *Journal of Intelligent & Robotic Systems*, vol. 61, pp. 85-101, 2011.

[3] T. W. Chun, Q. V. Tran, H. H. Lee, and H. G. Kim, "Sensorless Control of BLDC Motor Drive for an Automotive Fuel Pump Using a Hysteresis Comparator," *IEEE Transactions on Power Electronics*, vol. 29, pp. 1382-1391, 2014.

[4] S. Jianwen, D. Nolan, M. Teissier, and D. Swanson, "A novel microcontroller-based sensorless brushless DC (BLDC) motor drive for automotive fuel pumps," *IEEE Transactions on Industry Applications*, vol. 39, pp. 1734-1740, 2003.

[5] X. Huang, A. Goodman, C. Gerada, Y. Fang, and Q. Lu, "Design of a Five-Phase Brushless DC Motor for a Safety Critical Aerospace Application," *IEEE Transactions on Industrial Electronics*, vol. 59, pp. 3532-3541, 2012.

[6] X. Huang, A. Goodman, C. Gerada, Y. Fang, and Q. Lu, "A Single Sided Matrix Converter Drive for a Brushless DC Motor in Aerospace Applications," *IEEE Transactions on Industrial Electronics*, vol. 59, pp. 3542-3552, 2012.

[7] H. Kim, J. Son, and J. Lee, "A High-Speed Sliding-Mode Observer for the Sensorless Speed Control of a PMSM," *IEEE Transactions on Industrial Electronics*, vol. 58, pp. 4069-4077, 2011.

[8] F. Parasiliti, R. Petrella, and M. Tursini, "Sensorless speed control of a PM synchronous motor based on sliding mode observer and extended Kalman filter," in *Conference Record of the 2001 IEEE Industry Applications Conference. 36th IAS Annual Meeting (Cat. No.01CH37248)*, 2001, pp. 533-540 vol.1.

[9] C. S. Staines, C. Caruana, and R. Raute, "A Review of Saliency-based Sensorless Control Methods for Alternating Current Machines," *IEEJ Journal of Industry Applications*, vol. 3, pp. 86-96, 2014.

[10] K. Scicluna, C. S. Staines, and R. Raute, "Sensorless position control of a PMSM for steer-by-wire applications," in *2016 International Conference on Control, Decision and Information Technologies (CoDIT)*, 2016, pp. 046-051.

[11] U. V, S. Pola, and K. P. Vittal, "Recent Developments in Control Schemes of BLDC Motors," in *2006 IEEE International Conference on Industrial Technology*, 2006, pp. 477-482.

[12] L. Byoung-Kuk, K. Tae-Hyung, and M. Ehsani, "On the feasibility of four-switch three-phase BLDC motor drives for low cost commercial applications: topology and control," *IEEE Transactions on Power Electronics*, vol. 18, pp. 164-172, 2003.

[13] M. Lazor and M. Štulrajter, "Modified field oriented control for smooth torque operation of a BLDC motor," in *2014 ELEKTRO*, 2014, pp. 180-185.

[14] N. Matsui, "Sensorless PM brushless DC motor drives," *Industrial Electronics, IEEE Transactions on*, vol. 43, pp. 300-308, 1996.

SIMULINK MODELS

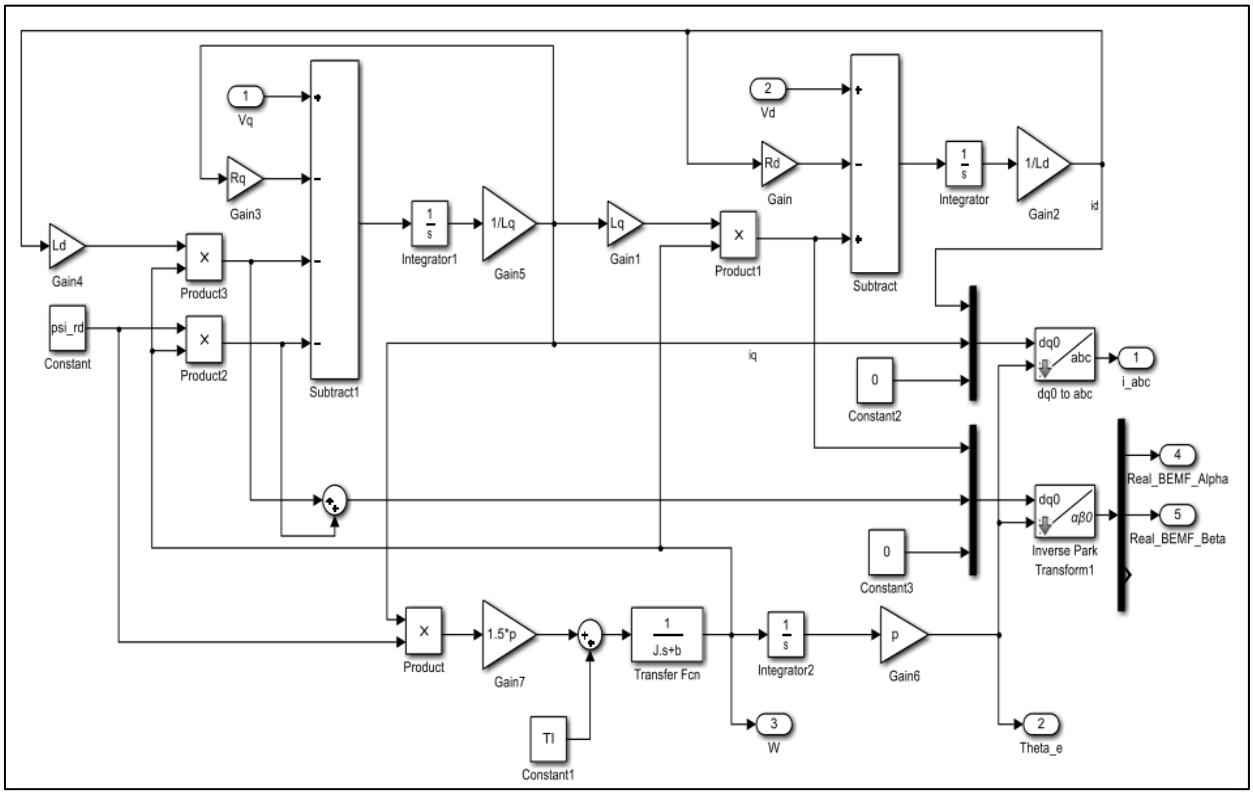

Model A. Simulink Model of BLDC Machine

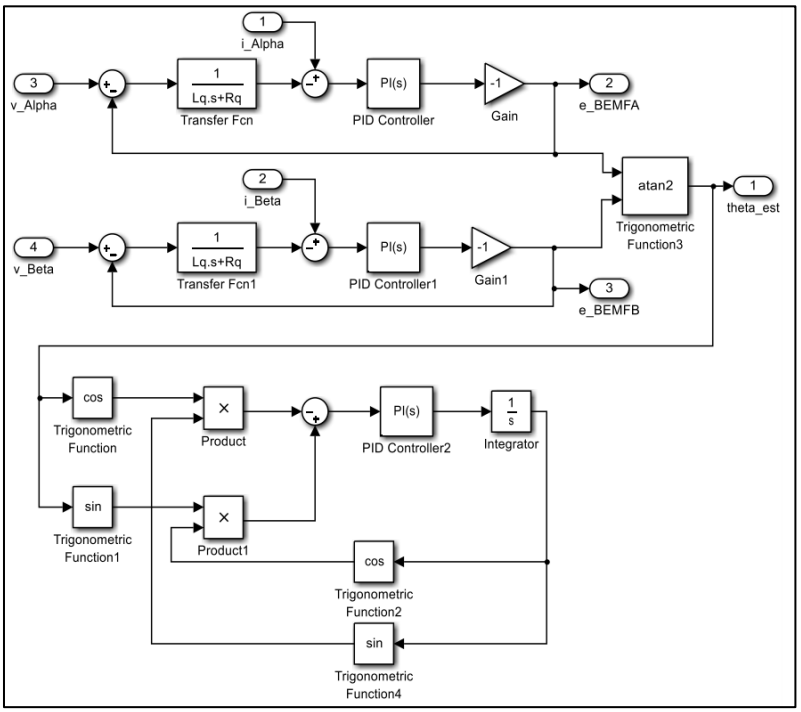

Model B. Simulink Model Based Sensorless Observer